Biochimica et Biophysica Acta 1808 (2011) 219–228

Contents lists available at ScienceDirect

Biochimica et Biophysica Acta

journal homepage: www.elsevier.com/locate/bbamem

Tryptophan orientations in membrane-bound gramicidin and melittin—a comparative linear dichroism study on transmembrane and surface-bound peptides

Frida R. Svensson [a], Per Lincoln [a], Bengt Nordén [a], Elin K. Esbjörner [b,*]

[a] Department of Chemical and Biological Engineering, Chalmers University of Technology, Kemivägen 10, SE-41296 Gothenburg, Sweden
[b] Department of Chemistry, University of Cambridge, Lensfield Road, Cambridge CB2 1EW, UK

ARTICLE INFO

Article history:
Received 28 May 2010
Received in revised form 20 September 2010
Accepted 8 October 2010
Available online 15 October 2010

Keywords:
Flow linear dichroism spectroscopy
Transition moment orientation
Ion-channel
Membrane-active peptide
Membrane interface

ABSTRACT

In the search for methods to study structure and function of membrane-associated proteins and peptides flow linear dichroism, LD, spectroscopy has emerged as a promising technique. Using shear-aligned lipid vesicles, conformations and binding geometries of membrane-bound bio-macromolecules can be assessed. Here we investigate anchoring properties and specific orientations of tryptophan relative to the peptide backbone and to the membrane normal for the model peptides gramicidin and melittin. We have monitored the conformational change associated with the refolding of non-channel gramicidin into its channel form, and quantitatively determined the average orientations of its tryptophan transition moments, suggesting that these residues adopt a well-defined orientation at the membrane interface. An important conclusion regards the structural variation of gramicidin between these two distinct transmembrane forms. Whilst circular dichroism (CD) spectra, as has been reported before, vary strongly between the two forms suggesting their structures might be quite different, the LD results clearly evidence both the peptide backbone orientation and tryptophan side-chain positioning to be very similar. The latter are oriented in accord with what is expected from their role to anchor peptide termini to the membrane surface. The variations in CD could be due to, the in LD observed, minor shifts in mutual orientation and distance between neighbouring tryptophans sensitively determining their exciton interactions. Our data dispute that the non-channel form of membrane-bound gramicidin would be any of the intertwined forms often observed in crystal as the positioning of tryptophans along the peptide axis would not be compatible with the strong interfacial positioning observed here. The general role of tryptophans as interfacial anchors is further assessed for melittin whose conformation shows considerable angular spread, consistent with a carpet model of its mechanism for induced membrane leakage, and a predominantly surface-aligned membrane orientation governed by amphipathic interactions.

1. Introduction

Biological membranes play a key role in sustaining life by compartmentalization of cells and their inner organelles. Whilst the basic component of membranes are lipids, between 20% and 75% of a membrane's mass is made up of proteins and up to 30% of the genes in our genomes encodes for integral membrane proteins [1]. These proteins participate in signalling and molecular transport across membranes, regulation of cellular function and response to external stimuli. The latter is strongly reflected in that approximately 60% of all currently used pharmaceuticals target membrane proteins [2]. However, despite their obvious importance for cellular function membrane proteins remain underrepresented in structural as well as biophysical studies and relatively little is known about the factors that drive their correct folding and function.

In this work we address differences between transmembrane and surface-oriented protein fragments using linear dichroism absorption spectroscopy to study orientations and alignment (binding geometry) of two model peptides bound to shear-aligned lipid vesicles. We have studied the antibiotic ion-channel gramicidin and the lytic peptide melittin as representatives of each orientation.

It is well established that tryptophan residues in membrane proteins are particularly abundant at the ends of membrane-spanning segments where they appear to function as "floats" holding the membrane protein at a correct position in the bilayer by positioning themselves firmly at the membrane interface [3,4]. Consequently,

Abbreviations: CD, circular dichroism; DOPC, 1,2-dioleoyl-*sn*-glycero-3-phosphocholine; DOPG, 1,2-dioleoyl-*sn*-glycero-3-phosphoglycerol; LD, linear dichroism; LD^r, reduced linear dichroism; LUV, Large unilamellar lipid vesicle; NMR, nuclear magnetic resonance; TEM, Thulstrup–Eggers–Michl's method

* Corresponding author. Tel.: +44 1223 336 366; fax: +44 1223 336362.
E-mail addresses: frida.svensson@chalmers.se (F.R. Svensson), lincoln@chalmers.se (P. Lincoln), norden@chalmers.se (B. Nordén), ee251@cam.ac.uk (E.K. Esbjörner).

0005-2736/$ – see front matter © 2010 Elsevier B.V. All rights reserved.
doi:10.1016/j.bbamem.2010.10.004

tryptophans are often crucial for both function and correct folding [5] and the physical basis for this interfacial preference has been explored by us [6] and others [7] using tryptophan model compounds. Here, we specifically address this question in a more complex context, to obtain a deeper understanding of the physical basis of the interfacial anchoring capacity of tryptophans, by investigating how tryptophan residues in these two model peptides align relative to the membrane and how the alignment of the peptide backbone may modulate their orientation. Gramicidin, a 15 residue hydrophobic peptide with alternating L- and D-amino acids from *Bacillus brevis*, can form cation-selective ion-channels spanning across lipid membranes by adopting a head-to-head β-helical dimer conformation in the bilayer [8,9] (see Fig. 1, right model). Despite its unusual backbone arrangement gramicidin has been extensively studied for its functions as a simplistic ion-channel (see reference [10] for a recent review). Gramicidin contains an unusual high number of tryptophans (four per monomer) and these residues, which in the channel form of gramicidin are positioned at the membrane interface, appear crucial for maintaining fold and function [5,11,12].

Melittin is a 26 residue lytic peptide, with a net positive charge and an amphipathic character. As the major component in honey bee venom [13] it displays potent lytic activities in most types of lipid membranes [14]. Upon binding to the membrane it adopts a partially α-helical structure perturbed by the proline residue at position 14 rendering the peptide in a conformation similar to a slightly bent rod [15]. It has been suggested that melittin would cause membrane damage by forming toroidal pores [16,17] but a surface-oriented "carpeting" model of membrane disruption appears more consistent with the bulk of existing experimental data (see references [18,19] and references therein). However, under certain experimental conditions, and particularly where aligned lipid multilayers have been used, melittin seem to have a tendency to adopt membrane-spanning configurations and thus the membrane orientation of melittin remains somewhat elusive warranting the further examination by linear dichroism spectroscopy described here [20].

Linear dichroism is the linearly polarized light counter-part to circular dichroism and gives information on the orientation of chromophores in a macroscopically aligned system. Flow linear dichroism applied to shear-aligned lipid vesicles have been used to provide both qualitative and quantitative detail of peptide-lipid interactions. The technique was developed by us some 10 years ago and has subsequently been used by us and others to determine the orientation of membrane bound organic dyes [21,22], membrane-active peptides [23–25], tryptophan side-chain derivatives [6] and membrane-associated peptides and proteins [26–30]. Although the information content in a linear dichroism spectroscopy experiment cannot compare with the atomistic detail obtained by high-resolution techniques such as X-ray crystallography and solution- and solid-state NMR [31–33], it has the advantage of being applicable to membrane proteins in a true and fully solvated lipid bilayer, and in that it provides orientational information with reference to the bilayer, information that is commonly lost in crystals. Further, since the LD technique is based on measuring the orientation of intrinsic protein chromophores it is easy to perform and not as susceptible to artefactual structural perturbations as for example spin-label electron paramagnetic resonance spectroscopy (EPR) [34] or fluorescence resonance transfer experiments requiring extrinsic labels. As we will show here, linear dichroism spectroscopy in combination with circular dichroism and tryptophan fluorescence techniques provide structural and orientational data that when assessed against high-resolution structural models of peptide and proteins acquired in solvent or membrane-mimetic micelles give important insight into their validity in a lipid bilayer.

Recently, Hicks et al. showed that linear dichroism may also be used to monitor the kinetics of gramicidin insertion into a lipid vesicle membrane opening possibilities to use LD to study membrane-induced protein folding [35]. Inspired by that finding we here provide a more detailed analysis of gramicidin in its membrane-bound state focusing on the refolding of gramicidin, induced by elevated temperature, from an initially adopted non-functional form in the membrane (usually assumed to be an antiparallel "intertwined" β-helix based on X-ray diffraction of gramicidin crystals prepared in various solvents) to the thermodynamically favoured conductive ion-channel which consists of a β-helix dimer (see Fig. 1). We are able to probe structural details of both conformations of gramicidin using a combination of linear and circular dichroism spectroscopy complemented by tryptophan fluorescence and show that LD is clearly sensitive enough to pick up small structural differences between these two states.

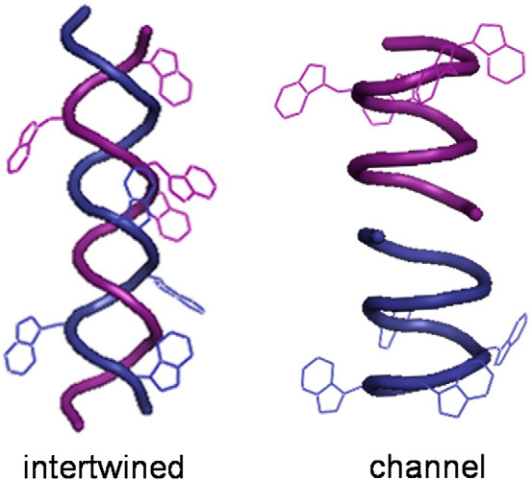

Fig. 1. Schematic picture of possible gramicidin conformations. The 3-D models were generated in PyMol using data from the Protein Data Bank. The intertwined conformation (left), with accession code 1alz, is an X-ray diffraction crystal structure obtained by crystallisation from ethanol [42]. The channel β-helix conformation (right), with accession code 1grm, is a structure obtained from NMR in SDS micelles [43].

2. Materials and methods

2.1. Materials

1,2-Dioleoyl-*sn*-glycero-3-phosphocholine (DOPC) and 1,2-dioleoyl-*sn*-glycero-3-phosphatidylglycerol (DOPG) were from Larodan (Malmö, Sweden). All-*trans*-retinoic acid, melittin (GIGAVLKVLTTGLPALIS-WIKRKRQQ-NH_2; 85% minimum purity, Phospholipase A_2 <5 units/mg solid), gramicidin (mixture of A, B and C containing 85% gramicidin A with the sequence HCO-V_LG$A_L$$L_D$$A_L$$V_D$$V_L$$V_D$$W_L$$L_D$$W_L$$L_D$$W_L$$L_D$$W_L$-NHC$H_2CH_2$OH), and sucrose were from Sigma. 10 mM potassium phosphate buffer (pH 7.4) with 50% (w/w) sucrose, prepared in deionised water was used unless else is stated.

2.2. Preparation of large unilamellar lipid vesicles

Large unilamellar lipid vesicles (LUVs) with a diameter of 100 nm were prepared by the extrusion technique. Briefly, lipids were dissolved in chloroform and mixed at desired molar ratios in a round bottom flask. The solvent was evaporated using a rotary evaporator under reduced pressure and remaining traces of solvent were thereafter removed by placing the flask with the lipid film under vacuum for at least 2 h. Vesicles were formed by dispersing the lipid film in buffer under vortexing followed by five freeze–thaw cycles (liquid nitrogen/37 °C) and extrusion 21 times through polycarbonate filters with 100 nm pore size using a LiposoFast-Pneumatic extruder (Avestin, Canada). Gramicidin was added to the lipid vesicles at the stage of preparation of the lipid film whereas melittin (dissolved at

high concentration in ethanol) was added directly to the lipid vesicle suspension in small aliquots.

2.3. Circular dichroism spectroscopy

CD spectra were recorded on a JASCO J-810 spectropolarimeter between 200 and 270 nm in 1 nm increments at room temperature using a 1 mm quartz cell. Ten scans were accumulated and averaged. All spectra were corrected for background contribution by subtracting spectra of the buffer. An exact reference for lipid vesicles cannot be obtained when the vesicles are prepared in presence of peptide. The lipid vesicles have, however, no appreciably CD on their own and contribution from light scattering were insignificant compared to the peptide CD at all wavelengths above 200 nm. CD are expressed as mean residue ellipticities $[\theta]_{MR}$ (deg cm^2/dmol).

2.4. Flow linear dichroism spectroscopy

Linear dichroism (LD) is defined as the differential absorption between orthogonal forms of plane polarized light, where the polarization vector of the incident light beam is oriented parallel and perpendicular to the orientation of the sample:

$$LD = A_{II} - A_{\perp} \quad (1)$$

Chromophores in a macroscopically aligned system will exhibit LD if their transition moments have a preferential orientation relative to the orientation axis of the system. Alignment of lipid vesicles can be achieved in an applied shear flow using a Couette flow cell device. The stationary laminar shear flow in the annular gap between the two concentric cylinders of the Couette cell will deform the lipid vesicles into slightly ellipsoidal shapes and align them with their induced long-axes parallel to the flow [21]. The reduced LD (LD^r), obtained by normalizing the LD with respect to the isotropic absorption of the sample, is directly related to the orientation of a particular transition moment. For lipid vesicles it is most convenient to define the orientation angles relative to the membrane normal (perpendicular to the orientation axis) since this is the unique axis in the system and because uniaxial distributions of orientations around this axis are expected. For a non-overlapping pure transition the LD^r is wavelength-independent and directly related to the orientation of the transition according to Eq. (2) [21]:

$$LD^r = \frac{LD}{A_{iso}} = \frac{3}{4}S\left(1 - 3\langle \cos^2 \alpha \rangle\right) \quad (2)$$

where $\langle \cos^2\alpha \rangle$ is the ensemble average and α represents the angle between the transition moment and the membrane normal. S is the orientation factor determined by the deformation and macroscopic orientation of the liposomes in the flow as well as the microscopic order of the lipid chains in the membrane [22].

LD spectra were recorded on a Jasco J-720 spectropolarimeter equipped with an Oxley prism to obtain linearly polarized light [36]. The lipid vesicles were oriented under a stationary shear flow of 3100 s^{-1} in an outer-rotating quartz Couette cell with a total path length of 1 mm. Spectra were recorded between 200 and 450 nm in 1 nm increments using a scan speed of 100 nm/min and a bandwidth of 2 nm. Three spectra were accumulated and averaged. Baselines, recorded on the same sample but without rotation of the Couette cell, were subtracted from all spectra. The spectropolarimeter records LD in ellipticity units (millidegrees) which were converted to differential absorbance units using the following relation [37]:

$$LD(\text{abs}) = \frac{4\pi\theta(\text{deg})}{180 \ln 10} = \frac{\theta(m\,\text{deg})}{32982} \quad (3)$$

For comparison, the differential absorbance was converted into molar absorptivity unit ε [M^{-1} cm^{-1}] by division with the peptide concentration in the sample and the path length of the Couette cell (1 mm). To enhance spectral quality we used dilute phosphate buffers (maximum transparency) supplemented with 50% (w/w) sucrose which reduces light scattering from the lipid vesicles by refractive index matching [23]. Additionally, the high sucrose content increase the viscous drag which results in higher degree of lipid vesicle deformation and hence better macroscopic alignment.

2.5. Analysis of LD spectra

We have previously shown that the orientation factor, S, of each aligned sample can be obtained using retinoic acid as an internal membrane probe [22]. Retinoic acid binds to lipid bilayers with high affinity and has one main well-defined transition moment along the long axis of the molecule. It inserts parallel to the lipid chains, i.e. perpendicular to the orientation axis, resulting in a negative LD signal around 350 nm. Using the fact that retinoic acid orients parallel to the lipid chains ($\alpha = 0°$) S can be calculated from the LD and the isotropic absorption of the sample at 350 nm (Eq. (2)). When the orientation parameter of the system is known, LD^r of membrane bound molecules can be used to determine orientation angles of transition moments relative the membrane normal [21,24,38].

The sign and magnitude of each absorption band in LD gives information on the orientation of that transition relative to the surface of the membrane and angular coordinates for the orientation of a certain transition can be obtained directly from LD^r if there is no spectral overlap in the relevant wavelength region. To resolve the individual contributions to LD from overlapping transitions (L_a and L_b in the case of tryptophan) we employed either the Thulstrup–Eggers–Michl's (TEM) method of step-wise reduction [39,40] or a spectral reconstruction by a linear combination approach [26]. TEM is particularly powerful to extract LD^r values from absorption bands with distinct features and has the advantage that no other reference spectra than the recorded absorption and LD of the sample are used. This method is originally based on stepwise "trial-and-error" formation of linear combinations of the polarized spectra (A_{II} and $A_{\perp}$). When a distinct spectral feature of the transition moment of interest disappears in this linear combination of the LD a reduction coefficient can be calculated and related to LD^r of that transition. The CD spectropolarimeter does not measure the polarized spectra separately but gives directly the differential spectra, the LD. We therefore use TEM directly on the LD and isotropic absorption spectra by forming linear combinations on the form $LD - kA_{iso}$. In this case the reduction coefficient, k, is directly equal to LD^r [41]. Alternatively we reconstructed the LD spectrum with help of previously recorded absorption spectra corresponding to the pure L_a and L_b absorption bands respectively using least-square analysis to find the best fit (Supplementary Fig. S1) [26]. The fraction of each reference spectrum that is needed to reconstruct the measured LD spectrum corresponds directly to LD^r if the absorbance of the sample matches the total absorbance of the L_a and L_b transitions.

2.6. Calculation of LD^r values and LD spectra from atomic resolution models of gramicidin

X-ray diffraction or NMR structures of one non-channel (pdb ID 1alz) and one channel (pdb ID 1grm) form of gramicidin were retrieved from the Protein Data Bank [42,43]. Average angular coordinates for the L_a and L_b transition moments of the tryptophan residues relative the helix axis were determined by approximating their moments with vectors between the closest atoms (see Fig. 2). LD curves were calculated from these values using reference spectra for the L_a and L_b absorption band (see Supplementary Fig. S1).

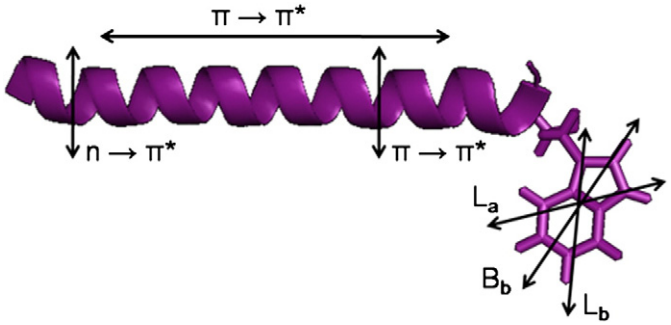

Fig. 2. Schematic picture of transition moment directions in an α-helical peptide with one tryptophan residue. The transition moment direction in gramicidin, which has an unusual β-helical fold, is discussed in the text. The peptide bond $\pi \rightarrow \pi^*$ transitions interact by exciton coupling and the lowest energy component (observable at 205–210 nm) is directed parallel to the helix axis. The highest energy component is oriented perpendicular to the helix axis and absorbs below 200 nm. The weak $n \rightarrow \pi^*$ is also perpendicular to the helix axis and may appear as a small shoulder on the red-edge of the $\pi \rightarrow \pi^*$ absorption band. The electronic transition moment directions in the indole chromophore of tryptophan are also depicted and further described in the text.

2.7. Peptide transition moments

Gramicidin and melittin contains respectively one and four tryptophan residues. The indole chromophore of tryptophan has three main electronic transitions giving rise to the B_b absorption band at 225 nm, the broad and unstructured L_a absorption band with maximum around 270 nm and the structured L_b absorption band with two conspicuous vibronic peaks just below 290 nm (Fig. 2). The peptide bond absorbs in the far UV region where the weak (electronically forbidden) $n \rightarrow \pi^*$ transition has the lowest energy. In an α-helix this transition is polarised perpendicular to the helix axis and may, if visible, appear as a shoulder near 220–230 nm on the considerably stronger absorption band of the low-energy exciton coupling of the $\pi \rightarrow \pi^*$ transition oriented parallel to the α-helix axis and centred around 210 nm. Gramicidin has an unusual backbone due to the alternating L- and D-amino acids in its sequence and the secondary structure is β-helical, i.e. a helical arrangement of β-sheets. The theoretical LD of gramicidin in the β-helical dimer channel form has been previously assessed using the coupled-oscillator model [23,44]. These calculations showed that in the channel form of gramicidin the highest energy exciton component of the $\pi \rightarrow \pi^*$ transition will be directed parallel to the channel axis, and a negative LD band below 200 nm is thus expected. Due to the strong overlap between the weak $n \rightarrow \pi^*$ transition and the considerably stronger B_b transition in tryptophan the former is commonly not visible in spectra where the B_b transition exhibits LD (i.e. where tryptophans are aligned) [37,45,46].

3. Results

3.1. Circular dichroism distinguishes non-channel from channel gramicidin

Gramicidin can adopt at least two functionally distinct transmembrane conformations in a lipid bilayer depending on the conditions, including type of solvent, under which the sample is prepared [47]. Here we focus on the structural details of the transition from a putative antiparallel intertwined transmembrane conformation, never structurally assigned in a membrane environment, but implied from structures obtained in solvent to be a non-conducting ion-channel, to the β-helix head-to-head dimer that is commonly accepted to be the functional ion-conducting channel form [48]. Starting from a sample where gramicidin is in a "non-channel" form it has previously been shown that gramicidin can refold into the thermodynamically more stable, and from experiment verified, channel form by incubation at elevated temperature (typically at least 60 °C) [47,49]. We prepared samples with gramicidin incorporated into 100 nm LUVs composed of DOPC lipids. They were obtained by dissolving gramicidin in chloroform and mixing it with the phospholipids (also in chloroform) before preparing a dry lipid film from which vesicles were reconstituted by dissolving the film in buffer. Circular and linear dichroism spectra were measured and the sample was then incubated at 65 °C for 15 h to allow for complete refolding of peptide into the channel form [48,50,51]. Thereafter new spectra were recorded on the same sample (see Fig. 3). The initial sample (purple line) gave rise to a CD spectrum (Fig. 3a) with a negative peak at 230 nm and a positive CD at shorter wavelengths as previously reported for non-channel gramicidin forms whereas the final sample (blue line) displayed maxima at 218 and 235 nm, a minimum at 230 nm and a negative CD band below 205 nm, which is typical for the channel form [47,49,52].

3.2. Linear dichroism of the non-channel and channel form of gramicidin reveals strong alignment of tryptophan side-chains

Samples of non-channel and channel forms of gramicidin in DOPC LUVs were aligned in shear flow to obtain linear dichroism (LD) spectra of the two conformations. Fig. 3b shows that gramicidin is well aligned (giving distinct LD signals) in both samples, as is expected for a transmembrane peptide or protein reconstituted into a lipid vesicle

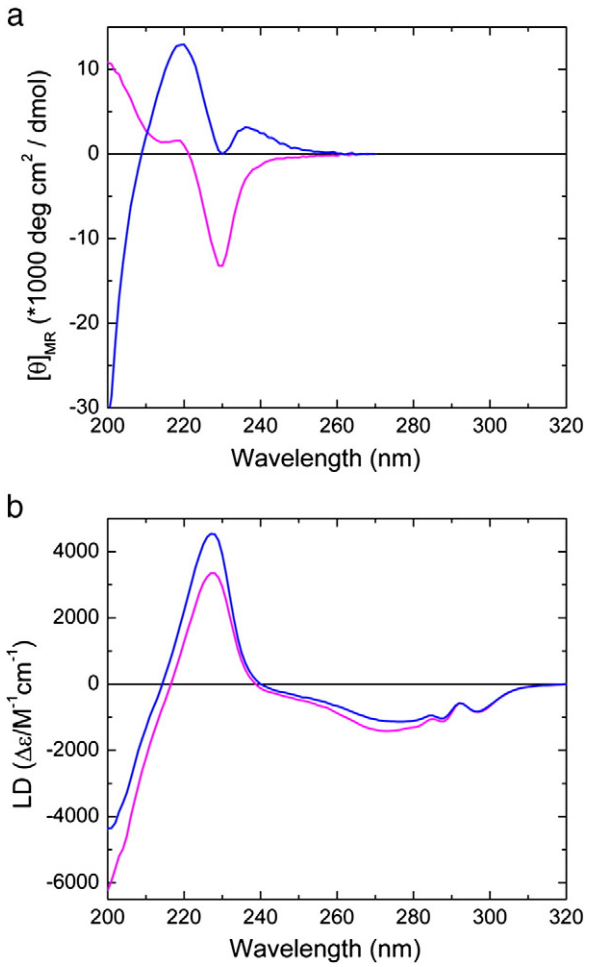

Fig. 3. Circular dichroism (a) and linear dichroism (b) spectra of membrane-bound gramicidin in non-channel form (purple) and channel form (blue). The spectra were recorded on gramicidin bound to DOPC lipid vesicles at a peptide-to-lipid molar ratio of 1:50 and a total lipid concentration 1.25 mM. Refolding of the non-channel form into the channel form was obtained by incubation of the sample at 65 °C for 15 h.

Table 1
Approximate wavelengths (λ) and molar extinction coefficients (ε) of the electronic transition moments in Fig. 2.

Transition	λ_{max} (nm)	ε (M^{-1} cm^{-1})
$n \rightarrow \pi^*$	225	100[a]
$\pi \rightarrow \pi^*$	~190	4–7000[a]
L_a	280	3800[b]
L_b	290	1900[b]
B_b	225	36000[b]

[a] Data from ref [40].
[b] Calculated from resolved excitation spectra of tryptophan (Supplementary Information, Fig. S1).

membrane. Notably, the two have rather similar LD spectra (Fig. 3b) despite their clearly different CD spectra (Fig. 3a). The peaks in the two LD spectra arise mainly from the aromatic tryptophan residues in gramicidin (four per monomer, eight per transmembrane entity). The negative peak at 275 nm is due to the L_a transition and the two sharp peaks with positive signature at 290 nm are due to the L_b transition (see Fig. 2 for transition moment directions). The positive peak at 225 nm is in a region of the spectrum where both tryptophan and the peptide bond absorb light (due to the B_b transition in tryptophan and the $n \rightarrow \pi^*$ transitions in each peptide bond). However, the $n \rightarrow \pi^*$ transitions are much weaker than the B_b transitions since each gramicidin monomer contains four tryptophans (ε ~144,000 M^{-1} cm^{-1} in total) and 14 peptide bonds (ε ~1,400 M^{-1} cm^{-1} in total); see Table 1 for a list of extinction coefficients (ε). Therefore, unless the tryptophans are aligned with their B_b transitions at orientations which are all extremely near 54.7° (the "magic angle" at which LD = 0) this absorption band must be dominated by tryptophan absorption, regardless the orientation of the peptide bond $n \rightarrow \pi^*$, which would in all cases only contribute marginally to the LD. The negative peak below 210 nm is due to the $\pi \rightarrow \pi^*$ transitions of the peptide backbone, and is in qualitative agreement with the calculated coupled-oscillator LD for β-helix gramicidin predicting the high energy exciton component of this transition to be negative for both β-helical dimers and anti-parallel intertwined β-helices [23]. In addition, these calculations suggest positive amplitude for the β-helical dimer in the low energy exciton component which may explain the slightly less negative LD displayed at 200–210 nm.

Despite the similarity between the two spectra there is a clear and reproducible difference in both magnitude and band shape of the LD spectra of the non-channel and channel forms, reflecting a distinct difference in tryptophan arrangement between the two conformations. At 225 nm the channel form (Fig. 3b; blue) has a somewhat stronger LD than the non-channel form (Fig. 3b; purple). Concomitantly, the negative LD at 275 nm decreases upon conversion to the channel form, and it is clear that the two spectra do not have exactly the same shape (see Supplementary Fig. S2 where the spectrum of the channel form was multiplied by a constant to make the value at 225 nm the same as the non-channel form which more clearly emphasize their different spectral shapes). The observed change is in agreement with a reorientation of one or several tryptophans upon transition from a non-channel form to the β-helix dimer channel. However, the change in orientation of the tryptophans is very small compared to what would be expected if the non-channel form were the intertwined helical dimer depicted in Fig. 1.

3.3. Linear dichroism of melittin

Fig. 4 shows linear dichroism spectra of melittin bound to neutral (DOPC) and net negatively charged (DOPC/DOPG) LUVs. The samples were prepared at a peptide-to-lipid ratio of 1:15 since melittin at these conditions has previously been suggested to insert in a transmembrane orientation in neutral membranes [20]. Spectra were recorded in buffer not containing Ca^{2+} and the trace amount

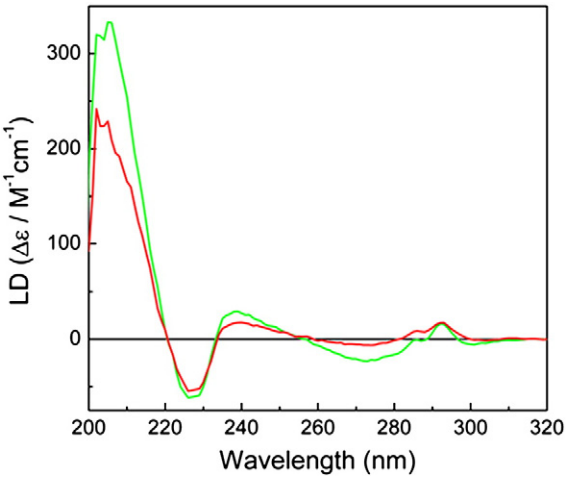

Fig. 4. Linear dichroism spectra of melittin in DOPC (red) and DOPC/DOPG (green) at a peptide to lipid molar ratio of 1:15 and a total lipid concentration of 1.25 mM.

of phospholipase A_2 present in our preparation should thus not be active [20] and in agreement with recent suggestions [53]. Despite that the spectra in Fig. 4 were recorded at extremely high peptide-to-lipid molar ratios (1:15) melittin did not cause complete lysis of the vesicles since the appearance of a LD signal requires that the membranes are alignable which in turn requires intact vesicles of a certain size. The two spectra in Fig. 4 have the same overall shape, indicating similarity in binding geometry for both the peptide backbone and the tryptophan residue at position 19. Melittin is α-helical when membrane-bound (see reference [54] and references therein and supplementary Fig. S3) and the positive LD from the peptide bond $\pi \rightarrow \pi^*$ transitions at 205 nm thus shows that melittin primarily binds along the surface of the membrane—a finding that supports previously suggested carpet models of leakage [18,19] where accumulation of peptide on the membrane surface results in weakening of membrane integrity and ruptures where a few peptides can transiently insert in a disordered fashion. The positive LD peak at 205–210 nm has been observed for several other membrane-active surface-oriented peptides and is the clearest LD hallmark for peptide backbone orientation [24–26].

Since melittin contains only one tryptophan residue, it is in principle possible to determine its unique orientation with high precision. Fig. 4 shows that this residue is oriented so that the L_b transition gives rise to a positive LD, as is the case for gramicidin in Fig. 3b. However, the two vibronic peaks are much broader indicating heterogeneity and the negative contribution from L_a is considerably smaller. The negative LD in the 225 nm absorption band shows clearly that the tryptophan B_b transition moment in melittin has a different orientation than the tryptophans in gramicidin. We observe a somewhat weaker signal in DOPC LUVs compared to DOPC/DOPG which could in principle be due to lower membrane affinity [55], but is more likely an effect of that neutral membranes are more easily destabilized than net negatively charged ones where the surface-bound state of melittin is stabilized by electrostatic interactions between positive peptide residues and negatively charge lipid head-groups. Membrane destabilization results in a higher degree of lipid disorder which in turn severely diminishes the degree of alignment in the LD experiment.

3.4. Calculation of tryptophan orientations from linear dichroism spectra

Using the spectral data in Fig. 3b together with the corresponding absorbance spectra of gramicidin in the non-channel and channel

Table 2
Orientation parameters for gramicidin and melittin in DOPC lipid vesicles. Orientation factors (S) were determined from the LD^r of an orientation probe molecule (retinoic acid). LD^r values were obtained from the spectra in Figs. 3b and 4 by estimating the contribution of each transition moment to the LD by spectral deconvolution. Insertion angles (α) were calculated using Eq. (2).

Peptide	S	Analysis[a]	Transition moment					
			L_a		L_b		B_b[b]	
			LD^r	α	LD^r	α	LD^r	α
Gramicidin (non-channel)	0.09	TEM	−0.047	41°	0.059	78°	–	~65°
Gramicidin (channel)	0.10	TEM	−0.041	44°	0.068	80°	–	~75°
Melittin	0.046	LS	−0.0125	48°	+0.02	68°	−0.0006	~51°

[a] The orientation of the L_a and L_b transition moments relative the membrane normal were calculated using least-square analysis (LS) or the step-wise reduction "trial-and-error" method as described in Materials and Methods.
[b] The B_b insertion angles for gramicidin were estimated using a 3D model of the tryptophan transitions.

samples we calculated the average orientation of the tryptophan side-chains in these two cases to obtain a quantitative measure of how the refolding affects tryptophan ring positioning relative to the membrane normal. Due to the spectral overlap the orientations of the L_a and L_b transition moments were obtained using the TEM method to separate the spectral contributions from each of these absorbing transitions to the LD spectrum, thereby obtaining their respective individual LD^r (see Materials and Methods and Supplementary Fig. S1). The angles for the B_b transition were assigned using a 3D model of the tryptophan transitions to determine its geometrically allowed orientations. Table 2 shows LD^r values, calculated orientation angles (α) and the overall macroscopic orientation (S) in each sample. S was obtained from LD recordings of the alignment of the membrane probe retinoic acid which was added to the samples after the peptide LD spectra had been taken (see Materials and Methods and Supplementary Fig. S4) [22]. The L_b transition has the most extreme LD^r, corresponding to an average angle of ~80° from the membrane normal, i.e. the transition is essentially parallel to the membrane surface. L_a shows a negative LD^r corresponding to a tilt of ~40° relative to the membrane normal. As a control of the correctness of LD^r values obtained using the spectral analysis described above we also employed a linear combination approach using previously measured absorption profiles for the L_a and L_b absorption bands [26] to fit the shape of the LD spectrum. This method yielded very similar results (see Supplementary Fig. S5 A).

The average orientation of the tryptophans in gramicidin, characterised by the orientations of the L_a, L_b, and B_b transition moments, is very similar to that previously obtained for several tryptophan side-chain analogs [6]. This indicates that the positioning of the tryptophans is strongly driven by their inherent preference for this particular orientation at the membrane interface, regardless of the detailed structure of its transmembrane peptide backbone.

The angular coordinates for melittin bound to a DOPC bilayer were determined using the linear combination analysis approach to deduce the relative contribution of L_a and L_b to the LD spectrum. The best fit is shown in Supplementary Fig. S5 B. The tryptophan residue in melittin adopts an average orientation that is closer to the magic angle (LD = 0) than the average orientations obtained for the four tryptophans in gramicidin suggesting a less precise alignment, i.e. greater angular flexibility, despite that melittin contains only one tryptophan residue.

3.5. Average tryptophan orientations from 3D atomic resolution models of non-channel and channel form of gramicidin

Using atomic coordinates deposited in the Protein Data Bank from X-ray crystal and NMR models of one proposed intertwined form [42], later associated with a transmembrane non-channel structure, and one β-helix dimer channel structure [43] of gramicidin (see Fig. 1) we computed the average orientations in these two structures, relative to the channel long-axis, of the tryptophan side-chains in these two models by approximating the L_b transition moment with a vector connecting the carbon atoms CG and CZ2, and the L_a transition moment with a vector between NE1 and CE3, atoms corresponding to Protein Data Bank file atom labelling. The angles are shown in Table 3. Using absorbance profiles for the pure L_a and L_b transitions obtained from the fluorescence anisotropy curve and fluorescence excitation spectrum of tryptophan in a 1,2-propandiol glass [26](see Supplementary Fig. S1 A) we also calculated hypothetical LD curves for these two structural models in the L_a/L_b absorption band (Fig. 5). The shapes obtained are in qualitative agreement with measured LD spectra in Fig. 3b but the L_b transition in the experimental spectrum has broader peaks than the corresponding hypothetical spectrum in Fig. 5 in agreement with the more heterogeneous environment in the former.

Table 3
Average orientation angles (α) (relative to the channel axis) for the tryptophan L_a and L_b transition moments in the two gramicidin models depicted in Fig. 1. Coordinates for the non-channel form (1alz) and the channel form (1grm) were retrieved from the Protein Data Bank.

	L_a	L_b
Non-channel	43°	57°
Channel	21°	81°

The orientation angles obtained for the examined channel form are in notable agreement with experimental data (see Table 3). The experimental value for the average L_a transition moment orientation is somewhat closer to the magic angle (54.7°, LD = 0) compared to the hypothetical, calculated from the NMR model which is probably a result of side-chain motion around the rotational axis of tryptophan. Since the L_a transition moment is almost perpendicular to this axis, it is reasonable to assume it will be particularly sensitive to rotational averaging which would in all cases occur on a much shorter time scale than the scan speed in the LD experiment. As expected, there is considerably less agreement in angular information between the experimental LD spectrum of the non-channel form and the calculated values from the intertwined model as the latter was derived from X-ray crystallography on gramicidin crystals grown in ethanol. This discrepancy was also noted by Hicks et al. when comparing their linear dichroism spectra of membrane-inserted gramicidin to a similar intertwined structural model [35].

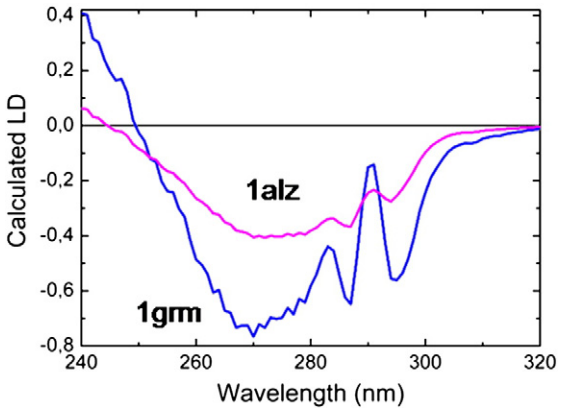

Fig. 5. Calculated LD spectra of gramicidin non-channel 1alz (purple) and channel 1grm (blue), corresponding to the models depicted in Fig. 1 obtained from the angular coordinates of the tryptophan side-chains in the respective models.

4. Discussion

4.1. The linear dichroism spectrum of the non-channel form of gramicidin is not consistent with an intertwined transmembrane model

Whilst the structure of the channel form of gramicidin is well recognized as a head-to-head dimer of two right-handed single-stranded β-helices [8,9,48] it is clear that gramicidin can also bind lipid bilayers as other types of dimers which are non-conducting and which can be distinguished from the channel form based on characteristic features in their CD spectra [56,57]. These structures have however not been assigned at atomic resolution in a membrane-mimetic environment. Nevertheless, the most frequently occurring suggestion in the literature is that it would form an anti-parallel intertwined helix of the type shown in Fig. 1 [56]. This is based on the experimental observation that the CD spectrum, and hence conformation of gramicidin in lipid vesicles, is dependent on the conformation it had in organic solvent prior to cosolubilisation with lipids [47]. Conformations with CD spectra characteristic of such anti-parallel intertwined helices have been isolated in a number of solvents including ethanol, methanol and 2-propanol [56,58,59].

We prepared gramicidin-containing lipid vesicles according to the procedures described by LoGrasso et al. [47] cosolubilising peptide and lipid in chloroform. The CD spectra in Fig. 3a verify the initial insertion of gramicidin in a non-channel conformation and the subsequent successful refolding into the channel form upon heating. However, despite these clear differences in CD indicative of a rearrangement from a non-channel conformation to the gramicidin channel the corresponding LD spectra show rather minor differences (Fig. 3b). Detailed analysis of the near-UV region of the LD spectrum made us conclude that the spectral difference corresponds to, in average for all tryptophan residues, a few degrees rotation of the indole plane. This is not consistent with the considerable difference in tryptophan orientation (and positioning) shown in the gramicidin models in Fig. 1 (see also Table 3). The main inconsistency is between the non-channel form and the anti-parallel intertwined helix where the proposed model deviates significantly from experimental data, strongly indicating that the intertwined form represented in Fig. 1 and found in crystals from ethanolic solvent is not consistent with the actual non-channel conformation in a lipid bilayer. As we will argue later, the LD is not only inconsistent with this particular intertwined model but with any intertwined model where the backbones of both monomers overlap along the entire length of the structure. By contrast, the tryptophan coordinates of the β-helical dimer agree reasonably well with the measured LD spectrum in Fig. 3b.

4.2. The positioning of the tryptophan residues in gramicidin is governed by their inherent preference for a specific orientation at the membrane interface

Consistent with the observation that the tryptophan orientations for the non-channel and channel form of gramicidin show small variations in tryptophan orientation are the similarity of the tryptophan emission from these two samples (supplementary Fig. S6) with wavelength maxima at 332.5 nm for the non-channel form and 331 nm for the channel form. Tryptophan emission is highly sensitive to polarity and the maximum of emission is hence a good indicator of the environment in which the tryptophans are embedded and our measurements indicate that the tryptophans are close to the membrane interface, but not inserted fully into the hydrocarbon core [60,61]. Further to this notion is the observation that the overall shape of the gramicidin LD spectra (with a strong maximum at 225 nm, a minimum at 270 nm and positive vibronic structure at 290 nm) is critically similar to what we have previously observed for the indole chromophore on its own incorporated into lipid vesicles [6]. Yau et al. have shown using NMR that indole resides intrinsically at the membrane interface due to the flat rigid shape and π electronic structure [7]. Thus it appears that gramicidin, both in the non-channel and channel conformation, strives to take on a conformation where the tryptophans can be accommodated at the membrane interface and can adopt an intrinsically preferred alignment. In the thermodynamically more stable channel form there is already a good hydrophobic match meaning that the tryptophans can arrange in clusters on either side of the membrane hydrocarbon core. By contrast, the tryptophans in the anti-parallel intertwined structure proposed by some to be the non-channel gramicidin form (Fig. 1) are more evenly spaced along the peptide backbone, and whilst this conformation may well be stable in organic solvent it is not consistent with our data as these suggest that tryptophans are in an interfacial position and not buried within the hydrocarbon core.

4.3. Features of the non-channel form of gramicidin

Based on the similarity of the LD spectra of the non-channel and channel form of gramicidin, consistency between tryptophan ring orientations in the β-helical dimer model and our measured channel form, the relationship between the LD spectra of gramicidin and the LD spectra of free indole at the membrane interface, and the tryptophan fluorescence data indicating interfacial positioning we suggest that the non-channel form of gramicidin cannot be any of the anti-parallel intertwined structures that have been determined from crystals grown in organic solvents as all these have their tryptophan residues spaced along the entire axis of the structure due to the full overlap of the backbones of the two monomers. However, the signs of the far-UV CD in Fig. 3 show that the non-channel form has an opposite backbone twist to that of the channel form and it thus not likely that the two forms of gramicidin that we have examined here are simply two related variants of the same β-helical dimer structure. Moreover, there is a significant energy barrier associated with the refolding of the initial non-channel form to structurally more well-defined channel form as the sample needs heating for several hours to fully convert. Further, the CD spectrum of our gramicidin preparation in solvent (Fig S7) is strongly resembling that of an anti-parallel intertwined structure early proposed by Veatch et al. [56] and with no apparent contribution from the other intertwined structures proposed by them. These above observations made us speculate on the nature of non-channel gramicidin in a lipid bilayer. Since gramicidin has previously been reported to have a "solvent history" [47] we find it reasonable to use the anti-parallel intertwined structure as a "starting structure". It is then possible, that the non-channel gramicidin is formed from the solvent-associated intertwined dimer directly upon incorporation into a lipid bilayer simply because of the strong preference of the many tryptophan residues to reside at the membrane interface rather than in the interior of the hydrocarbon core. Indeed, gramicidin mutants with tryptophan residues replaced with phenylalanines have been shown to adopt thermodynamically stable intertwined conformations in lipid bilayers [62,63] supporting our hypothesis that it is the putative positioning of tryptophans in the hydrophobic interior of the lipid bilayer that prohibits gramicidin from adopting intertwined structures of the type, depicted in Fig. 1, in a lipid bilayer.

A possible non-channel form that would be consistent with our data is an extended, partially intertwined structure where the backbone of the two monomer units are intertwined in the hydrocarbon core and where the C-terminal part of the backbone arrange probably in a helical manner near the membrane surface so that the tryptophans can reside at the interface in their preferred orientation.

It has been suggested that intertwined and β-helical dimers will exist in equilibrium. In such a situation the CD spectrum at any given time point during the conversion of gramicidin from non-channel to channel should be a linear combination of the true spectra of each of these two forms [50]. To explore whether our data could be explained

by such equilibrium between two distinct structures, rather than by a model of the type we speculate above, we measured the CD spectrum on gramicidin in ethanol to obtain a reference spectrum for the intertwined conformation depicted in Fig. 1. We then fitted the CD spectrum of the membrane-bound "non-channel" form as a linear combination of the channel-form spectrum and the spectrum in ethanol (Supplementary Fig. S7). If an equilibrium of intertwined and β-helical dimer structures of the types depicted in Fig. 1 would exist our analysis suggests that these would be populated in approximately equal proportions. This would mean that 25% of the tryptophans in our "non-channel" samples reside within the hydrophobic core of the membrane, with an orientation different from that at the interface and with a considerably shorter wavelength of maximum fluorescence. Our LD and fluorescence data do not support such conclusion.

We then asked ourselves how different the two conformations we have examined by LD and CD really are given their similar LD spectra. There is substantial evidence from solid state ^{15}N NMR that gramicidin adopts two distinct backbone conformations in DMPC bilayers, the first being consistent with the β-helical dimer channel whereas the second could not be assigned but was reported to vanish upon heat-incubation of the sample [64], suggesting this could hold true for our case. Further, the CD spectra at short wavelengths, where absorption is mainly from the peptide backbone, have opposite signs indicating differences in backbone helicity. This, as mentioned above, points to that the non-channel structure has the left-handed twist that has been observed for the non-channel form in crystals prepared in ethanol. The quite particular and clearly different shapes of the gramicidin CD spectra suggest that whilst tryptophan orientations relative the membrane normal are largely similar between the non-channel and channel form there is a distinct difference in their arrangement relative to one another. The gramicidin CD arises from exciton coupling between aligned tryptophan B_b transitions. This coupling is extremely sensitive to the exact relative orientations and distances between the coupling transition moments (for example if the tryptophan rings arrange head-to-head, if they stack or if they are at an angle to one another). All these possibilities are compatible with them having the same orientation relative to the membrane normal since LD is the same for transition moments that are uniaxially distributed relative to the reference axis. The substantial observed difference in CD is thus not necessarily representing a major difference in actual conformation of the two gramicidin forms. Instead, small changes in the symmetry of tryptophan alignment at the membrane interface are likely. It appears from the magnitude and shape of the CD spectra in Fig. 3a that both forms have the same exciton signature albeit less pronounced for the non-channel form. This could for example mean that the rim of the non-channel has a larger diameter than the rim of the channel form. Nevertheless it is worth noting that drawing conclusions about the conformational changes in gramicidin based on CD alone may exaggerate the differences between these conformations.

4.4. The binding of melittin to lipid bilayers is heterogeneous and consistent with a carpet model of leakage

The LD analysis of melittin in neutral DOPC and negatively charged DOPC/DOPG lipid vesicles inconclusively suggests that the binding mode is similar in both cases and that the α-helical parts of the peptide backbone are mainly oriented parallel to the membrane surface. The magnitude of the LD signals are however weak compared to what one would expect from a peptide with high α-helical content, and the heterogeneity in environment around and orientation of the tryptophan residue indicate that also the peptide backbone can explore a range of orientations relative to the membrane normal. This is in agreement with a carpet model of membrane leakage where disordered insertion of peptides can occur upon weakening of the lipid bilayer due to peptide accumulation at the surface [18,19,65].

It is remarkable that the average orientation of the four individual tryptophans in each monomer of gramicidin adopts a more homogeneous orientation with respect to the membrane normal than the sole tryptophan in melittin and this finding in combination with that the α-helical part of the peptide backbone is overall surface-oriented indicate strongly that melittin does not form stable pore-like entities as is the case for gramicidin. Further, the LD spectrum of tryptophan in melittin is clearly different from that of the tryptophans in gramicidin suggesting that the positioning of tryptophan in melittin is so strongly influenced by the amphipathic interactions of the entire peptide that its own preferential orientation cannot be fulfilled.

It has been suggested that at a peptide-to-lipid ratio (P/L) of 1/15 melittin adopts a transmembrane orientation in zwitterionic vesicles, whereas negatively charged lipids stabilizes the surface bound orientation [14,66]. Further, Hristova et al. suggested from oriented CD, that melittin starts to reorient from the membrane-parallel orientation to a transmembrane conformation at a P/L = 1/25 in DOPC lipid vesicles [67] and Yang et al. found, also by oriented CD, that 68% of melittin in POPC vesicle at P/L = 1/15 is perpendicular to the bilayer [20]. We have thus assessed melittin at conditions that have been reported to favour stable transmembrane insertion or pore-formation. As mentioned above, if a substantial fraction of melittin would insert into the membrane the LD peak at 205–210 nm must change sign or at least approach zero as the orientation of the α-helix would be orthogonal to that of the surface-bound peptide. In addition, it follows from Eq. (2) that a transition moment oriented parallel to the membrane normal has a negative LD that is twice the magnitude of a transition moment with identical oscillator strength oriented perpendicular to the membrane normal and experimental observation indicates that transmembrane peptides are always considerably more well-aligned than surface-oriented ones (due to them being in a more anisotropic environment, compare for example the spectral magnitudes in Fig. 6). Thus, even a relatively small population of melittin in a stable pore conformation would reduce the LD in the 205–210 nm peak significantly. This is not observed.

We do see that the LD is somewhat lower for melittin in neutral lipid bilayers compared to the net negatively charged ones, but because the LD signal decreases equally much in all absorption bands this is more consistent with either a weaker binding affinity [55] or a decrease in overall alignment due to the membrane disruptive effects on the microscopic order in each vesicle. In conclusion, melittin is largely surface-oriented in our experiment but, due to its lytic activities via a carpet-like mechanism, heterogeneity exists and a

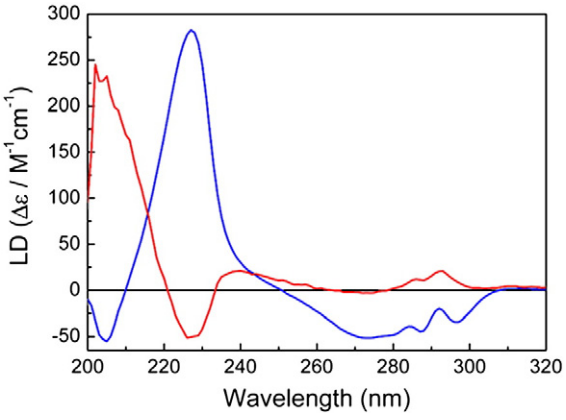

Fig. 6. Linear dichroism spectra of gramicidin in the channel form (blue) incorporated in DOPC lipid vesicles at a peptide-to-lipid molar ratio of 1:50 (the spectra has been divided by five to obtain comparable magnitudes) and melittin (red) at a peptide-to-lipid molar ratio of 1:15. The total lipid concentration was 1.25 mM.

fraction of the peptides may transiently insert. The data are nevertheless inconsistent with pore-formation.

4.5. Comparison of the preferred tryptophan orientations in gramicidin and melittin gives new views on the physical basis of tryptophans interfacial anchoring properties

In Fig. 6 we have plotted the LD spectra for melittin (blue) and gramicidin (red) to allow for direct comparison of their respective spectral characteristics. The melittin LD spectrum has several features that we find typical for peptides that bind parallel to the membrane surface [24,26] including positive signature at 210 nm and a negative peak at 225 nm. Gramicidin on the other hand has an LD spectrum similar to that of indole [6] with features that are clearly different to those of melittin, including much stronger signals, sharper features in the 250–300 nm region and a positive peak at 225 nm. We propose that these spectral features, mainly stemming from the particular orientation of tryptophans, is an inherent characteristic related to backbone orientation and that peptides can be assigned as surface-oriented or transmembrane on the basis of how their tryptophans align relative to the membrane normal. It is clear that the positioning of tryptophans in gramicidin is completely driven by the preference of these residues for the membrane interface, in agreement with their proposed function as 'floats' for integral membrane proteins keeping these in a functional position within the membrane [3,4,7]. Equally clear is the absence of this preferred orientation for the single tryptophan residue in melittin, indicating that the exact alignment of tryptophans in a surface-oriented peptide is not governed solely by their interfacial preference. Instead our data suggest that secondary amphipathicity and electrostatic interactions between charged side-chains and lipid head-groups have a more decisive role on the positioning of such peptides. The negative sign of the B_b absorption band at 225 nm show that tryptophan in melittin find an orientation where the pseudo long axis is oriented towards the membrane normal. This indicates that whilst this residue cannot adopt its intrinsic orientation it strives to position itself with the most hydrophobic part of the side-chain towards the membrane interior and the electronegative nitrogen towards the polar head-groups providing some additional new insight into the molecular basis for tryptophan's interplay at the membrane interface.

Acknowledgments

This work was supported by grants from the Lennander foundation (E.K.E.), the Wenner-Gren Foundations (long-term post-doctoral fellowship to E.K.E), the Swedish Research Council (B.N.) and the European Commission (B.N).

Appendix A. Supplementary data

Supplementary data to this article can be found online at doi:10.1016/j.bbamem.2010.10.004.

References

[1] E. Wallin, G. von Heijne, Genome-wide analysis of integral membrane proteins from eubacterial, archaean, and eukaryotic organisms, Protein Sci. 7 (1998) 1029–1038.
[2] M.A. Yildirim, K.I. Goh, M.E. Cusick, A.L. Barabasi, M. Vidal, Drug-target network, Nat. Biotechnol. 25 (2007) 1119–1126.
[3] M.R. de Planque, B.B. Bonev, J.A. Demmers, D.V. Greathouse, R.E. Koeppe, F. Separovic, A. Watts, J.A. Killian, Interfacial anchor properties of tryptophan residues in transmembrane peptides can dominate over hydrophobic matching effects in peptide–lipid interactions, Biochemistry 42 (2003) 5341–5348.
[4] M. Schiffer, C.H. Chang, F.J. Stevens, The functions of tryptophan residues in membrane proteins, Protein Eng. 5 (1992) 213–214.
[5] W. Hu, K.C. Lee, T.A. Cross, Tryptophans in membrane proteins: indole ring orientations and functional implications in the gramicidin channel, Biochemistry 32 (1993) 7035–7047.
[6] E.K. Esbjörner, C.E. Caesar, B. Albinsson, P. Lincoln, B. Nordén, Tryptophan orientation in model lipid membranes, Biophys. Res. Commun. 361 (2007) 645–650.
[7] W.M. Yau, W.C. Wimley, K. Gawrisch, S.H. White, The preference of tryptophan for membrane interfaces, Biochemistry 37 (1998) 14713–14718.
[8] D.W. Urry, M.C. Goodall, J.D. Glickson, D.F. Mayers, The gramicidin A transmembrane channel: characteristics of head-to-head dimerized (L, D) helices, Proc. Natl. Acad. Sci. U. S. A. 68 (1971) 1907–1911.
[9] S. Weinstein, B.A. Wallace, E.R. Blout, J.S. Morrow, W. Veatch, Conformation of gramicidin A channel in phospholipid vesicles: a 13C and 19F nuclear magnetic resonance study, Proc. Natl. Acad. Sci. U. S. A. 76 (1979) 4230–4234.
[10] D.A. Kelkar, A. Chattopadhyay, The gramicidin ion channel: a model membrane protein, Biochim. Biophys. Acta 1768 (2007) 2011–2025.
[11] R.E. Koeppe, O.S. Anderson, Engineering the gramicidin channel, Annu. Rev. Biophys. Biomol. Struct. 25 (1996) 231–258.
[12] H. Sun, D.V. Greathouse, O.S. Andersen, R.E. Koeppe, The preference of tryptophan for membrane interfaces: insights from n-methylation of tryptophans in gramicidin channels, J. Biol. Chem. 283 (2008) 22233–22243.
[13] E. Habermann, Bee and wasp venoms, Science 177 (1972) 314–322.
[14] S. Ohki, E. Marcus, D.K. Sukumaran, K. Arnold, Interaction of melittin with lipid membranes, Biochim. Biophys. Acta 1194 (1994) 223–232.
[15] H. Vogel, F. Jahnig, The structure of melittin in membranes, Biophys. J. 50 (1986) 573–582.
[16] D. Allende, S.A. Simon, T.J. McIntosh, Melittin-induced bilayer leakage depends on lipid material properties: evidence for toroidal pores, Biophys. J. 88 (2005) 1828–1837.
[17] D. Sengupta, H. Leontiadou, A.E. Mark, S.J. Marrink, Toroidal pores formed by antimicrobial peptides show significant disorder, Biochim. Biophys. Acta 1778 (2008) 2308–2317.
[18] H. Raghuraman, A. Chattopadhyay, Orientation and dynamics of melittin in membranes of varying composition utilizing NBD fluorescence, Biophys. J. 92 (2007) 1271–1283.
[19] B. Bechinger, K. Lohner, Detergent-like actions of linear amphipathic cationic antimicrobial peptides, Biochim. Biophys. Acta 1758 (2006) 1529–1539.
[20] L. Yang, T.A. Harroun, T.M. Weiss, L. Ding, H.W. Huang, Barrel-stave model or toroidal model? A case study on melittin pores, Biophys. J. 81 (2001) 1475–1485.
[21] M. Ardhammar, N. Mikati, B. Nordén, Chromophore orientation in liposome membranes probed with flow dichroism, J. Am. Chem. Soc. 120 (1998) 9957–9958.
[22] F.R. Svensson, P. Lincoln, B. Nordén, E.K. Esbjörner, Retinoid chromophores as probes of membrane lipid order, J. Phys. Chem. B 111 (2007) 10839–10848.
[23] M. Ardhammar, P. Lincoln, B. Nordén, Invisible liposomes: refractive index matching with sucrose enables flow dichroism assessment of peptide orientation in lipid vesicle membrane, Proc. Natl. Acad. Sci. U. S. A. 99 (2002) 15313–15317.
[24] C.E. Brattwall, P. Lincoln, B. Nordén, Orientation and conformation of cell-penetrating peptide penetratin in phospholipid vesicle membranes determined by polarized-light spectroscopy, J. Am. Chem. Soc. 125 (2003) 14214–14215.
[25] C.E. Caesar, E.K. Esbjörner, P. Lincoln, B. Nordén, Membrane interactions of cell-penetrating peptides probed by tryptophan fluorescence and dichroism techniques: correlations of structure to cellular uptake, Biochemistry 45 (2006) 7682–7692.
[26] E.K. Esbjörner, K. Oglecka, P. Lincoln, A. Gräslund, B. Nordén, Membrane binding of pH-sensitive influenza fusion peptides. Positioning, configuration, and induced leakage in a lipid vesicle model, Biochemistry 46 (2007) 13490–13504.
[27] C.E. Caesar, E.K. Esbjörner, P. Lincoln, B. Nordén, Assigning membrane binding geometry of cytochrome C by polarized light spectroscopy, Biophys. J. 96 (2009) 3399–3411.
[28] J. Rajendra, A. Damianoglou, M. Hicks, P. Booth, P.M. Rodger, A. Rodger, Quantitation of protein orientation in flow-oriented unilamellar liposomes by linear dichroism, Chem. Phys. 326 (2006) 210–220.
[29] S.M. Ennaceur, M.R. Hicks, C.J. Pridmore, T.R. Dafforn, A. Rodger, J.M. Sanderson, Peptide adsorption to lipid bilayers: slow processes revealed by linear dichroism spectroscopy, Biophys. J. 96 (2009) 1399–1407.
[30] M.R. Hicks, A. Damianoglou, A. Rodger, T.R. Dafforn, Folding and membrane insertion of the pore-forming peptide gramicidin occur as a concerted process, J. Mol. Biol. 383 (2008) 358–366.
[31] M. Hong, Structure, topology, and dynamics of membrane peptides and proteins from solid-state NMR spectroscopy, J. Phys. Chem. B 111 (2007) 10340–10351.
[32] S.J. Opella, NMR and membrane proteins, Nat. Struct. Biol. 4 (Suppl) (1997) 845–848.
[33] E. Strandberg, P. Tremouilhac, P. Wadhwani, A.S. Ulrich, Synergistic transmembrane insertion of the heterodimeric PGLa/magainin 2 complex studied by solid-state NMR, BBA Biomembr. 1788 (2009) 1667–1679.
[34] D. Marsh, Orientation and peptide–lipid interactions of alamethicin incorporated in phospholipid membranes: polarized infrared and spin-label EPR spectroscopy, Biochemistry 48 (2009) 729–737.
[35] M.R. Hicks, A. Damianoglou, A. Rodger, T.R. Dafforn, Folding and membrane insertion of the pore-forming peptide gramicidin occur as a concerted process, J. Mol. Biol. 383 (2008) 358–366.
[36] B. Nordén, M. Kubista, T. Kurucsev, Linear dichroism spectroscopy of nucleic acids, Q. Rev. Biophys. 25 (1992) 51–170.
[37] A. Rodger, B. Nordén, Circular Dichroism and Linear Dichroism, Oxford University Press, Oxford, 1997.
[38] A. Rodger, J. Rajendra, R. Marrington, M. Ardhammar, B. Norden, J.D. Hirst, A.T.B. Gilbert, T.R. Dafforn, D.J. Halsall, C.A. Woolhead, C. Robinson, T.J.T. Pinheiro, J. Kazlauskaite, M. Seymour, N. Perez, M.J. Hannon, Flow oriented linear dichroism

to probe protein orientation in membrane environments, Phys. Chem. Chem. Phys. 4 (2002) 4051–4057.
[39] J. Michl, E.W. Thulstrup, J.H. Eggers, Polarization spectra in stretched polymer sheets. Physical significance of the orientation factors and determination of p–p*transition moment directions in molecules of low symmetry, J. Phys. Chem. 74 (1970) 3878–3884.
[40] E.W. Thulstrup, J. Michl, J.H. Eggers, Polarization spectra in stretched polymer sheets. II. Separation of p–p* absorption of symmetrical molecules into components, J. Phys. Chem. 74 (1970) 3868–3878.
[41] P. Lincoln, A. Broo, B. Norden, Diastereomeric DNA-binding geometries of intercalated ruthenium(II) trischelates probed by linear dichroism: [Ru(phen)(2)dppz](2+) and [Ru(phen)(2)bdppz](2+), J. Am. Chem. Soc. 118 (1996) 2644–2653.
[42] B.M. Burkhart, R.M. Gassman, D.A. Langs, W.A. Pangborn, W.L. Duax, Heterodimer formation and crystal nucleation of gramicidin D, Biophys. J. 75 (1998) 2135–2146.
[43] A.L. Lomize, V. Orekhov, A.S. Arsen'ev, Refinement of the spatial structure of the gramicidin A ion channel, Bioorg. Khim. 18 (1992) 182–200.
[44] P.M. Bayley, E.B. Nielsen, J.A. Schellman, The rotatory properties of molecules containing two peptide groups: theory, J. Phys. Chem. 73 (1969) 228–243.
[45] J. Brahms, J. Pilet, H. Damany, V. Chandrasekharan, Application of a new modulation method for linear dichroism studies of oriented biopolymers in the vacuum ultraviolet, Proc. Natl. Acad. Sci. U. S. A. 60 (1968) 1130–1137.
[46] C.R. Cantor, P.R. Schimmel, Biophysical Chemistry. Part II, W. H. Freeman and Co, San Francisco, 1980.
[47] P.V. LoGrasso, F. Moll III, T.A. Cross, Solvent history dependence of gramicidin A conformations in hydrated lipid bilayers, Biophys. J. 54 (1988) 259–267.
[48] A.S. Arseniev, I.L. Barsukov, V.F. Bystrov, A.L. Lomize, A. Ovchinnikov Yu, 1H-NMR study of gramicidin A transmembrane ion channel. Head-to-head right-handed, single-stranded helices, FEBS Lett. 186 (1985) 168–174.
[49] J.A. Killian, K.U. Prasad, D. Hains, D.W. Urry, The membrane as an environment of minimal interconversion. A circular dichroism study on the solvent dependence of the conformational behavior of gramicidin in diacylphosphatidylcholine model membranes, Biochemistry 27 (1988) 4848–4855.
[50] M.C. Bano, L. Braco, C. Abad, A semi-empirical approach for the simulation of circular dichroism spectra of gramicidin A in a model membrane, Biophys. J. 63 (1992) 70–77.
[51] D.A. Kelkar, A. Chattopadhyay, Monitoring ion channel conformations in membranes utilizing a novel dual fluorescence quenching approach, Biochem. Biophys. Res. Commun. 343 (2006) 483–488.
[52] S.S. Rawat, D.A. Kelkar, A. Chattopadhyay, Monitoring gramicidin conformations in membranes: a fluorescence approach, Biophys. J. 87 (2004) 831–843.
[53] A. Damianoglou, A. Rodger, C. Pridmore, T.R. Dafforn, J.A. Mosely, J.M. Sanderson, M.R. Hicks, The synergistic action of melittin and phospholipase A2 with lipid membranes: development of linear dichroism for membrane-insertion kinetics, Protein Pept. Lett. 17 (11) (2010) 1351–1362.
[54] H. Raghuraman, A. Chattopadhyay, Melittin: a membrane-active peptide with diverse functions, Biosci. Rep. 27 (2007) 189–223.
[55] T.H. Lee, H. Mozsolits, M.I. Aguilar, Measurement of the affinity of melittin for zwitterionic and anionic membranes using immobilized lipid biosensors, J. Pept. Res. 58 (2001) 464–476.
[56] W.R. Veatch, E.T. Fossel, E.R. Blout, The conformation of gramicidin A, Biochemistry 13 (1974) 5249–5256.
[57] D.V. Greathouse, J.F. Hinton, K.S. Kim, R.E. Koeppe II, Gramicidin A/short-chain phospholipid dispersions: chain length dependence of gramicidin conformation and lipid organization, Biochemistry 33 (1994) 4291–4299.
[58] D.J. Laird, M.M. Mulvihill, J.A. Lillig, Membrane-induced peptide structural changes monitored by infrared and circular dichroism spectroscopy, Biophys. Chem. 145 (2009) 72–78.
[59] S.V. Sychev, N.A. Nevskaya, S. Jordanov, E.N. Shepel, A.I. Miroshnikov, V.T. Ivanov, The solution conformations of gramicidin-a and its analogs, Bioorg. Chem. 9 (1980) 121–151.
[60] G. Beschiaschvili, J. Seelig, Peptide binding to lipid-membranes—spectroscopic studies on the insertion of a cyclic somatostatin analog into phospholipid-bilayers, Biochim. Biophys. Acta 1061 (1991) 78–84.
[61] J.R. Lakowicz, Principles of Fluorescence Spectroscopy, 2nd ed. Springer, Singapore, 2006.
[62] M. Cotten, F. Xu, T.A. Cross, Protein stability and conformational rearrangements in lipid bilayers: linear gramicidin, a model system, Biophys. J. 73 (1997) 614–623.
[63] D. Salom, E. Perez-Paya, J. Pascal, C. Abad, Environment- and sequence-dependent modulation of the double-stranded to single-stranded conformational transition of gramicidin A in membranes, Biochemistry 37 (1998) 14279–14291.
[64] J.A. Killian, L.K. Nicholson, T.A. Cross, Solid-state 15N-NMR evidence that gramicidin A can adopt two different backbone conformations in dimyristoylphosphatidylcholine model membrane preparations, Biochim. Biophys. Acta 943 (1988) 535–540.
[65] X. Zhang, K. Oglecka, S. Sandgren, M. Belting, E.K. Esbjörner, B. Nordén, A. Gräslund, Dual functions of the human antimicrobial peptide LL-37—target membrane perturbation and host cell cargo delivery, BBA Biomembranes 1798 (2010) 2201–2208.
[66] A.S. Ladokhin, S.H. White, "Detergent-like" permeabilization of anionic lipid vesicles by melittin, Biochim. Biophys. Acta 1514 (2001) 253–260.
[67] K. Hristova, C.E. Dempsey, S.H. White, Structure, location, and lipid perturbations of melittin at the membrane interface, Biophys. J. 80 (2001) 801–811.